LOD-MS for Gross-Pitaevskii Equation in Bose-Einstein Condensates

Linghua Kong[1,*], Jialin Hong[2] and Jingjing Zhang[3]

[1] *School of Mathematics and Information Science, Jiangxi Normal University, Nanchang, Jiangxi 330022, P.R. China.*
[2] *State Key Laboratory of Scientific and Engineering Computing, Institute of Computational Mathematics and Scientific/Engineering Computing, Academy of Mathematics and System Science, Chinese Academy of Sciences, P.O. Box 2719, Beijing 100190, P.R. China.*
[3] *School of Mathematics and Information Science, Henan Polytechnic University, Jiaozuo, Henan 454000, P.R. China.*

Abstract. The local one-dimensional multisymplectic scheme (LOD-MS) is developed for the three-dimensional (3D) Gross-Pitaevskii (GP) equation in Bose-Einstein condensates. The idea is originated from the advantages of multisymplectic integrators and from the cheap computational cost of the local one-dimensional (LOD) method. The 3D GP equation is split into three linear LOD Schrödinger equations and an exactly solvable nonlinear Hamiltonian ODE. The three linear LOD Schrödinger equations are multisymplectic which can be approximated by multisymplectic integrator (MI). The conservative properties of the proposed scheme are investigated. It is mass-preserving. Surprisingly, the scheme preserves the discrete local energy conservation laws and global energy conservation law if the wave function is variable separable. This is impossible for conventional MIs in nonlinear Hamiltonian context. The numerical results show that the LOD-MS can simulate the original problems very well. They are consistent with the numerical analysis.

1 Introduction

The existence of the Bose-Einstein Condensate (BEC) was predicted in the early 1920s by Bose and Einstein. It was experimentally created and confirmed until 1995 in atomic

---

*Corresponding author. *Email addresses:* `konglh@mail.ustc.edu.cn` (L. Kong), `hjl@lsec.cc.ac.cn` (J. Hong), `zhangjj@hpu.edu.cn` (J. Zhang)

gas at ultra low temperature [7]. The BEC phenomena can be reported by the mean-field theory in physics and can be modeled by the well-known Gross-Pitaevskii (GP) equation [9,18]

$$ i\hbar u_t = -\frac{\hbar^2}{2m}\nabla^2 u + \overline{V}_d(\mathbf{x})u + \frac{4\pi\hbar^2 a_s}{m}|u|^2 u, \quad \mathbf{x}\in\mathbb{R}^d, \ t\geqslant 0, \tag{1.1} $$

where m is the atomic mass, $\hbar$ is the Planck constant, a_s is the s-wave scatting length ($a_s > 0$ for repulsive interaction and $a_s < 0$ for attractive interaction), and $\overline{V}_d(\mathbf{x})$ is the external potential imposed on the physical system.

For convenience, it is necessary to scale GP equation (1.1) into the dimensionless form

$$ i u_t = -\frac{1}{2}\nabla^2 u + V_d(\mathbf{x})u + \beta_d|u|^2 u, \quad \mathbf{x}\in\mathbb{R}^d, \ t\geqslant 0, \tag{1.2} $$

where β_d is a real constant, and $V_d(\mathbf{x})$ is the external potential acting on the physical system which can be periodic

$$ V_d(\mathbf{x}) = \begin{cases} 1-\sin^2 x, & d=1, \\ 1-\sin^2 x\sin^2 y, & d=2, \\ 1-\sin^2 x\sin^2 y\sin^2 z, & d=3, \end{cases} $$

or harmonic

$$ V_d(\mathbf{x}) = \begin{cases} \frac{\gamma_x^2 x^2}{2}, & d=1, \\ \frac{\gamma_x^2 x^2+\gamma_y^2 y^2}{2}, & d=2, \\ \frac{\gamma_x^2 x^2+\gamma_y^2 y^2+\gamma_z^2 z^2}{2}, & d=3, \end{cases} $$

with the trapped frequencies $\gamma_x,\gamma_y,\gamma_z$ in x-, y- and z-direction, respectively.

We consider the Cauchy problem of GP equation (1.2) with the initial value

$$ u(\mathbf{x},0) = u^0(\mathbf{x}), \quad \mathbf{x}\in\mathbb{R}^d. \tag{1.3} $$

By direct calculation, one can derive that the GP equation (1.2)-(1.3) endows with the following two important invariants: the first one is mass invariant

$$ \mathcal{Q}(t) = \int_{\mathbb{R}^d}|u(\mathbf{x},t)|^2 d\mathbf{x} = \int_{\mathbb{R}^d}|u(\mathbf{x},0)|^2 d\mathbf{x} = \mathcal{Q}(0), \tag{1.4} $$

and the second one is energy invariant

$$ \mathcal{E}(t) = \int_{\mathbb{R}^d}\left[\frac{1}{2}|\nabla u(\mathbf{x},t)|^2 + V_d(\mathbf{x})|u|^2 + \frac{\beta_d}{2}|u|^4\right]d\mathbf{x} = \mathcal{E}(0). \tag{1.5} $$

Significant progress on numerical simulation of BEC phenomena has been made over the last ten years (see [2–4,8,14,20,23,24,27] and references therein). In [2–4], Bao et al.

presented time-splitting spectral methods for various GP equation with different boundary conditions. Zhang et al. designed local absorbing boundary conditions for GP equation combined with split-step method [26]. Du and Ju [8] developed a finite volume method for the Ginzburg-Landau model. Tian et al. [23] considered a completely implicit multisymplectic structure-preserving scheme for GP equation with vortices. However, the partition of the considered domain must be crude because of the limitation of the performance of computer. Islas et al. proposed a multisymplectic spectral method for the GP equation [14], but it is very difficult in practical computing. Ruprecht et al. [20] simulated the ground state solution and dynamics of GP equations by Crank-Nicolson scheme. In [24], Wang presented a split-step difference scheme for GP equation.

Splitting technique has different names in different subjects. It is fractional-step method in computational fluid dynamics, split-step method in optics, acoustics and nonlinear PDEs, dimensional splitting, alternative directional method and local one-dimensional (LOD) method in multidimensional PDEs, etc. In multidimensional context, it was originally developed for multidimensional parabolic equations by Douglas et al. [16, 17], including alternative direction implicit (ADI) method, LOD method. It was generalized to nonlinear KdV equations by Tappert [22] which split the KdV equations into purely linear and nonlinear subproblems. Now, it is widely employed for solving nonlinear PDEs for its simplicity and flexibility, including the GP equation [24]. The method has also been successfully applied to symplectic geometric integrators [10].

Multisymplectic integrators (MIs) preserving multisymplectic geometric structure are favorable and applied to many mathematical and physical dynamics (see [1,5,6,12,13,19, 25] and references therein). As is well-known, for general multisymplectic Hamiltonian system, there are no explicit MIs. Therefore, it is rather difficult to establish an efficient and approachable MI for multidimensional Hamiltonian systems ($d \geq 2$ for instance). To wipe off the flaw, recently, we developed a novel kind of splitting MIs for intricate or multidimensional Hamiltonian PDEs (MHPDEs) [11,15]. The method makes neither nonlinear iterative nor expensive algebraic systems. The basic thought of the method is to decompose the original MHPDEs into several LOD HPDEs. Then we approximate them by MIs, which preserve discrete LOD multisymplectic conservation laws. We call the method LOD-MS for multidimensional MHPDEs. In this paper, we investigate LOD-MS for the GP equation (1.2).

The general 3D MHPDE reads

$$Mz_t + \sum_{j=1}^{3} K_j z_{x_j} = \nabla_z S(z), \tag{1.6}$$

where M, K_j ($j = 1, 2, 3$) are skew-symmetric matrices, and $S(z)$ is a smooth function which is called Hamiltonian function. It is easy to derive that the multisymplectic system (1.6) satisfies the following local conservation laws:

- Multisymplectic conservation law (MCL)

$$\frac{\partial}{\partial t}\omega + \sum_{j=1}^{3}\frac{\partial}{\partial x_j}\kappa_j = 0,$$

with the symplectic density and symplectic fluxes

$$\omega = d\mathbf{z}\wedge Md\mathbf{z}, \quad \kappa_j = d\mathbf{z}\wedge K_j d\mathbf{z}, \quad j=1,2,3.$$

- Local energy conservation law (LECL)

$$\frac{\partial}{\partial t}E(\mathbf{z}) + \nabla\cdot\mathbf{F}(\mathbf{z}) = 0,$$

where the energy density $E(\mathbf{z})$ and energy flux $\mathbf{F}(\mathbf{z})$ are

$$E(\mathbf{z}) = S(\mathbf{z}) - \frac{1}{2}\sum_{j=1}^{3}\mathbf{z}^T K_j \mathbf{z}_{x_j}, \quad \mathbf{F}(\mathbf{z}) = (F_1, F_2, F_3)^T,$$

$$F_j(\mathbf{z}) = \frac{1}{2}\mathbf{z}^T K_j \mathbf{z}_t, \, j=1,2,3.$$

The local conservation laws suggest that the density and fluxes can vary from time to time and from point to point. Nevertheless, the density increment in time must be equal to the flux increment at every space point.

The outline of the paper is planned as follows: In Section 2, we give a brief overview on the splitting method and multisymplectic Runge-Kutta (RK) methods. Section 3 is about the multisymplectic structure and its LOD multisymplectic structure of the GP equation (1.2). The conservation laws of the structures are discussed in the section. In Section 4, based on the established LOD multisymplectic structure of the GP equation in Section 3, we develop LOD-MS I and LOD-MS II. The splitting error of the former is of first-order and the latter is of second-order. The conservative properties and stability of the LOD-MS are investigated in Section 5. In Section 6, some numerical examples are reported to verify the numerical behavior of the new developed LOD-MS. Finally, some conclusions and remarks come into being in Section 7.

2   Review of splitting methods and Runge-Kutta type MIs

As we know that one can only construct explicit partitioned RK type MIs for separable MHPDEs [19]. However, most MHPDEs are inseparable. In other words, we can only construct completely implicit MIs for them. In consideration of stability, implicit schemes are superior to explicit ones. In this section, we give a brief review for the splitting methods and the RK type MIs.

Firstly, we give a short retrospection of the splitting method. The basic point in splitting method is to decouple the original mathematical model into a group of appropriate subproblems. Then one solves the subproblems in a given sequence approximately or accurately. The solver of the preceding subproblem is employed as the initial value of the rear. The mathematical description of the thought is as follows. Consider the initial value problem

$$\begin{cases} \dfrac{\partial}{\partial t} u(t) = \mathcal{A}u(t) = (\mathcal{L} + \mathcal{N})u(t), \\ u(0) = u_0, \end{cases} \tag{2.1}$$

where $\mathcal{A}, \mathcal{L}$ and $\mathcal{N}$ are spatial operators. The formal solution of the initial value problem (2.1) is

$$u(t) = \exp(t\mathcal{A})u_0 = \exp(t(\mathcal{L} + \mathcal{N}))u_0. \tag{2.2}$$

The computational of exponential operator $\exp(t(\mathcal{L} + \mathcal{N}))$ is very difficult or very expensive regularly. However, the exponential operators $\exp(t\mathcal{L})$ and $\exp(t\mathcal{N})$, which are formal solution operators of the simpler procedures

$$\frac{\partial}{\partial t} u(t) = \mathcal{L}u(t), \tag{2.3}$$

$$\frac{\partial}{\partial t} u(t) = \mathcal{N}u(t), \tag{2.4}$$

respectively, may be computed either more easily or accurately. We resolve the simpler problems (2.3) and (2.4) in a given sequence instead of solving the original problem (2.1) directly. Generally speaking, $\exp(t(\mathcal{L} + \mathcal{N})) \neq \exp(t\mathcal{L})\exp(t\mathcal{N})$ due to the non-commutativity between $\mathcal{L}$ and $\mathcal{N}$. Suppose τ be the time step size, $t^n = n\tau$, the two frequently used sequences are:

- First-order version: Lie-Trotter splitting

$$\begin{aligned} u(t^n) = \exp(\tau(\mathcal{L} + \mathcal{N}))u(t^{n-1}) &\approx \exp(\tau\mathcal{L})\exp(\tau\mathcal{N})u(t^{n-1}) \\ &\approx [\exp(\tau\mathcal{L})\exp(\tau\mathcal{N})]^n u_0. \end{aligned} \tag{2.5}$$

- Second-order version: Strang splitting [21]

$$\begin{aligned} u(t^n) &\approx \exp\left(\frac{\tau}{2}\mathcal{L}\right)\exp(\tau\mathcal{N})\exp\left(\frac{\tau}{2}\mathcal{L}\right)u(t^{n-1}) \\ &\approx \exp\left(\frac{\tau}{2}\mathcal{L}\right)\exp(\tau\mathcal{N})\exp(\tau\mathcal{L})\exp(\tau\mathcal{N})\exp\left(\frac{\tau}{2}\mathcal{L}\right)u(t^{n-2}) \\ &\approx \exp\left(\frac{\tau}{2}\mathcal{L}\right)[\exp(\tau\mathcal{N})\exp(\tau\mathcal{L})]^{n-1}\exp(\tau\mathcal{N})\exp\left(\frac{\tau}{2}\mathcal{L}\right)u_0. \end{aligned} \tag{2.6}$$

By the Baker-Campbell-Hausdorf (BCH) formula, the time-splitting error of the first version (2.5) and the second version (2.6) are of first-order and second-order, respectively.

An s-stage RK method for a general Hamiltonian system

$$\frac{d}{dt}\mathbf{z} = J\nabla_{\mathbf{z}}H(\mathbf{z}), \tag{2.7}$$

is

$$\begin{cases} K^j = \mathbf{z}^n + \tau \sum_{l=1}^{s} a_{jl} J\nabla_{\mathbf{z}} H(K^l), & j=1,2,\cdots,s, \\ \mathbf{z}^{n+1} = \mathbf{z}^n + \tau \sum_{j=1}^{s} b_j J\nabla_{\mathbf{z}} H(K^j), \end{cases} \tag{2.8}$$

where J is the standard symplectic matrix, and τ is the step length of the method, $H(z)$ is the Hamiltonian function, and a_{jl}, b_j are undetermined weighted factors.

Proposition 2.1 ([10]). An s-stage RK method (2.8) for (2.7) is symplectic if

$$a_{lj}b_l + a_{jl}b_j - b_l b_j = 0, \quad \text{for any } l,j = 1,2,\cdots,s. \tag{2.9}$$

For $s=1$, one has the midpoint rule

$$\mathbf{z}^{n+1} = \mathbf{z}^n + \tau J\nabla_{\mathbf{z}} H\left(\mathbf{z}^{n+1/2}\right), \quad \text{where } \mathbf{z}^{n+1/2} = \frac{1}{2}(\mathbf{z}^n + \mathbf{z}^{n+1}), \tag{2.10}$$

which is symplectic.

For a general one-dimensional multisymplectic Hamiltonian system

$$M\mathbf{z}_t + K\mathbf{z}_x = \nabla_{\mathbf{z}} S(\mathbf{z}), \tag{2.11}$$

where M and K are skew-symmetric matrices, and $S(\mathbf{z})$ is some smooth functional, concatenating a pair of symplectic RK integrators in space and time directions, it results in a MI [19]. For example, if one discretizes the system (2.11) by a pair of midpoint rules (2.10) it achieves

$$M\delta_t \mathbf{z}_{j+1/2}^{n+1/2} + K\delta_x \mathbf{z}_{j+1/2}^{n+1/2} = \nabla_{\mathbf{z}} S(\mathbf{z}_{j+1/2}^{n+1/2}), \tag{2.12}$$

where $\delta_s \mathbf{z}_{j+1/2}^{n+1/2}$ is the centered quotient in the s-direction with s being either x or t, and

$$\mathbf{z}_{j+1/2}^{n+1/2} = \frac{1}{2}\left(\mathbf{z}_{j+1}^{n+1/2} + \mathbf{z}_j^{n+1/2}\right) = \frac{1}{4}\left(\mathbf{z}_{j+1}^{n+1} + \mathbf{z}_{j+1}^n + \mathbf{z}_j^{n+1} + \mathbf{z}_j^n\right).$$

The midpoint scheme (2.12) is multisymplectic, that is to say, it satisfies the discrete MCL [5, 19]

$$\frac{\omega_{j+1/2}^{n+1} - \omega_{j+1/2}^n}{\tau} + \frac{\kappa_{j+1}^{n+1/2} - \kappa_j^{n+1/2}}{h} = 0. \tag{2.13}$$

For simplicity, we set the spatial domain be $[0,h]^3$, that is, the spatial index $(j,k,l) :\equiv (0,0,0)$. For the 3D Hamiltonian system (1.6), one can devise MIs for it, such as the centered box scheme [19]

$$M\delta_t \mathbf{z}^{n+\frac{1}{2}}_{\frac{1}{2},\frac{1}{2},\frac{1}{2}} + \sum_{m=1}^{3} K_m \delta_{x_m} \mathbf{z}^{n+\frac{1}{2}}_{\frac{1}{2},\frac{1}{2},\frac{1}{2}} = \nabla_{\mathbf{z}} S\left(\mathbf{z}^{n+\frac{1}{2}}_{\frac{1}{2},\frac{1}{2},\frac{1}{2}} \right), \tag{2.14}$$

where $\delta_s \mathbf{z}^{n+1/2}_{\frac{1}{2},\frac{1}{2},\frac{1}{2}}$ is the centered quotient in the s-direction with s being either x_1,x_2,x_3 or t, and $\mathbf{z}^n_{j,k,l}$ is an approximation of function $\mathbf{z}(x_1,x_2,x_3,t)$ at node $(x_{1j},x_{2k},x_{3l},t^n)$. However, this scheme is rather inefficient and resource consuming. In a manner, it is inapproachable due to the limitation of the power of computer. We turn to the LOD-MS [15].

For general cases, it is very hard in establishing approachable MIs for the MHPDE (1.6) as what was alleged previously. We split them into several LOD MHPDEs as follows:

$$\overline{M}\overline{\mathbf{z}}_t + \overline{K}_j \overline{\mathbf{z}}_{x_j} = \nabla_{\overline{\mathbf{z}}} S_j(\overline{\mathbf{z}}), \quad j=1,2,3, \tag{2.15}$$

where $S_1(\overline{\mathbf{z}}) + S_2(\overline{\mathbf{z}}) + S_3(\overline{\mathbf{z}}) = S(\mathbf{z})$, and $\overline{M}, \overline{K}_j$ and $\overline{\mathbf{z}}$ may be either the same as those in (1.6) or different from them. This can be observed from [11, 15]. It is obvious that the LOD HPDEs (2.15) fulfill the LOD MCLs and LOD LECLs

$$\frac{\partial}{\partial t}\omega + \frac{\partial}{\partial x_j}\kappa_j = 0, \quad j=1,2,3, \tag{2.16}$$

$$\frac{\partial}{\partial t}E + \frac{\partial}{\partial x_j}F_j = 0, \quad j=1,2,3. \tag{2.17}$$

Certainly, one can further decompose one or more of the LOD MHPDEs (2.15) into simpler ones if necessary, such as linear subproblem and nonlinear subproblem [11].

3   Multisymplectic structure for GP equation

In this section, we investigate the multisymplectic structure and LOD multisymplectic formulation for the 3D GP equation,

$$iu_t = [L+N(V,|u|^2)]u = (L_x+L_y+L_z)u + N(V,|u|^2)u, \tag{3.1}$$

where $L_x = -\frac{1}{2}\partial_{xx}$, $L_y = -\frac{1}{2}\partial_{yy}$, $L_z = -\frac{1}{2}\partial_{zz}$ are linear differential operators, and $N(V,|u|^2) = V(x,y,z) + \beta|u|^2$ is a nonlinear operator.

To reformulate the GP equation (3.1) into the form (1.6), we suppose $u = p+iq$ and introduces the conjugate momenta $p_x = v$, $q_x = w$, $p_y = \varphi$, $q_y = \psi$, $p_z = \zeta$, $q_z = \eta$. Thus, the

GP equation can be cast into the multisymplectic Hamiltonian system,

$$
\begin{cases}
-q_t + \dfrac{1}{2}(v_x + \varphi_y + \zeta_z) = V(x,y,z)p + \beta(p^2 + q^2)p, \\[2mm]
p_t + \dfrac{1}{2}(w_x + \psi_y + \eta_z) = V(x,y,z)q + \beta(p^2 + q^2)q, \\[2mm]
-\dfrac{1}{2}p_x = -\dfrac{1}{2}v, \qquad -\dfrac{1}{2}q_x = -\dfrac{1}{2}w, \\[2mm]
-\dfrac{1}{2}p_y = -\dfrac{1}{2}\varphi, \qquad -\dfrac{1}{2}q_y = -\dfrac{1}{2}\psi, \\[2mm]
-\dfrac{1}{2}p_z = -\dfrac{1}{2}\zeta, \qquad -\dfrac{1}{2}q_z = -\dfrac{1}{2}\eta,
\end{cases}
\tag{3.2}
$$

with $\mathbf{z} = [p,q,v,w,\varphi,\psi,\zeta,\eta]^T$, and the skew-symmetric matrices

$$
M = \begin{bmatrix} J_4 & \mathbf{0}_4 \\ \mathbf{0}_4 & \mathbf{0}_4 \end{bmatrix}, \quad
K_1 = \frac{1}{2}\begin{bmatrix} L_4 & \mathbf{0}_4 \\ \mathbf{0}_4 & \mathbf{0}_4 \end{bmatrix}, \quad
K_2 = \frac{1}{2}\begin{bmatrix} \mathbf{0}_4 & C_4 \\ -C_4 & \mathbf{0}_4 \end{bmatrix}, \quad
K_3 = \frac{1}{2}\begin{bmatrix} \mathbf{0}_4 & D_4 \\ -D_4 & \mathbf{0}_4 \end{bmatrix}.
$$

Here

$$
J_4 = \begin{bmatrix} 0 & -1 & 0 & 0 \\ 1 & 0 & 0 & 0 \\ 0 & 0 & 0 & 0 \\ 0 & 0 & 0 & 0 \end{bmatrix}, \quad
L_4 = \begin{bmatrix} \mathbf{0}_2 & I_2 \\ -I_2 & \mathbf{0}_2 \end{bmatrix}, \quad
C_4 = \begin{bmatrix} I_2 & \mathbf{0}_2 \\ \mathbf{0}_2 & \mathbf{0}_2 \end{bmatrix}, \quad
D_4 = \begin{bmatrix} \mathbf{0}_2 & I_2 \\ \mathbf{0}_2 & \mathbf{0}_2 \end{bmatrix},
$$

where I_n and $\mathbf{0}_n$ are $n \times n$ identity matrix and zeros matrix, respectively.

The Hamiltonian function is

$$
S(\mathbf{z}) = \frac{1}{4}\left[2V(x,y,z)(p^2+q^2) + \beta(p^2+q^2)^2 - (v^2 + w^2 + \varphi^2 + \psi^2 + \zeta^2 + \eta^2) \right].
$$

By straightforward calculation, the symplectic structures are

$$
\omega = dq \wedge dp, \qquad\qquad \kappa_1 = \frac{1}{2}(dp \wedge dv + dq \wedge dw),
$$

$$
\kappa_2 = \frac{1}{2}(dp \wedge d\varphi + dq \wedge d\psi), \quad \kappa_3 = \frac{1}{2}(dp \wedge d\zeta + dq \wedge d\eta),
$$

and the energy density and energy fluxes are

$$
E(\mathbf{z}) = 2V(x,y,z)(p^2+q^2) + \beta(p^2+q^2)^2 + (v^2 + w^2 + \varphi^2 + \psi^2 + \zeta^2 + \eta^2),
$$
$$
F_1(\mathbf{z}) = -2(p_t v + q_t w), \quad F_2(\mathbf{z}) = -2(p_t \varphi + q_t \psi), \quad F_3(\mathbf{z}) = -2(p_t \zeta + q_t \eta).
$$

As was stated previously, it was very difficult in developing practical MIs for the non-separable MHPDE (3.2). In view of the importance of MI, we split (3.2) into the following

LOD PDEs

$$iu_t = -\frac{1}{2}u_{xx} = L_x u, \tag{3.3}$$

$$iu_t = -\frac{1}{2}u_{yy} = L_y u, \tag{3.4}$$

$$iu_t = -\frac{1}{2}u_{zz} = L_z u, \tag{3.5}$$

$$iu_t = [V(x,y,z) + \beta|u|^2]u = N(V,|u|^2)u. \tag{3.6}$$

The LOD PDEs (3.3), (3.4), (3.5) can be written in the LOD multisymplectic formulation

$$J_4\frac{\partial}{\partial t}\mathbf{z}_j + L_4\frac{\partial}{\partial x_j}\mathbf{z}_j = \nabla_{\overline{\mathbf{z}}_j}S_j(\overline{\mathbf{z}}_j), \quad j=1,2,3, \tag{3.7}$$

where $x_1 = x$, $x_2 = y$, $x_3 = z$, and $\overline{\mathbf{z}}_1 = (p,q,v,w)^T$, $\mathbf{z}_2 = (p,q,\varphi,\psi)^T$, $\overline{\mathbf{z}}_3 = (p,q,\zeta,\eta)^T$, with the Hamiltonian functions

$$S_1(\overline{\mathbf{z}}) = -\frac{1}{4}(v^2+w^2), \quad S_2(\overline{\mathbf{z}}) = -\frac{1}{4}(\varphi^2+\psi^2), \quad S_3(\overline{\mathbf{z}}) = -\frac{1}{4}(\zeta^2+\eta^2).$$

The nonlinear subproblem (3.6) degenerates to the Hamiltonian formulation

$$\frac{d}{dt}\hat{\mathbf{z}} = J^{-1}\nabla_{\hat{\mathbf{z}}}H(\hat{\mathbf{z}}), \quad \forall x,y,z, \tag{3.8}$$

where

$$\hat{\mathbf{z}} = (p,q)^T, \quad J = \begin{bmatrix} 0 & -1 \\ 1 & 0 \end{bmatrix},$$

and the Hamiltonian function is

$$H(\hat{\mathbf{z}}) = \frac{1}{4}[2V(x,y,z)(p^2+q^2) + \beta(p^2+q^2)^2].$$

Accordingly, the LOD MHPDEs (3.3), (3.4), (3.5), (3.6) satisfy the following LOD MCLs

$$\frac{\partial}{\partial t}(dq \wedge dp) + \frac{\partial}{\partial x}(dp \wedge dv + dq \wedge dw) = 0, \quad \forall y,z, \tag{3.9}$$

$$\frac{\partial}{\partial t}(dq \wedge dp) + \frac{\partial}{\partial y}(dp \wedge d\varphi + dq \wedge d\psi) = 0, \quad \forall x,z, \tag{3.10}$$

$$\frac{\partial}{\partial t}(dq \wedge dp) + \frac{\partial}{\partial z}(dp \wedge d\zeta + dq \wedge d\eta) = 0, \quad \forall x,y, \tag{3.11}$$

$$\frac{d}{dt}(dq \wedge dp) = 0, \qquad\qquad \forall x,y,z,t, \tag{3.12}$$

respectively, and the LOD LECLs

$$\frac{\partial}{\partial t}E_1 + \frac{\partial}{\partial x}F_1 = \frac{\partial}{\partial t}(v^2+w^2) - 2\frac{\partial}{\partial x}(vp_t+wq_t) = 0, \quad \forall y,z, \tag{3.13}$$

$$\frac{\partial}{\partial t}E_2 + \frac{\partial}{\partial y}F_2 = \frac{\partial}{\partial t}(\varphi^2+\psi^2) - 2\frac{\partial}{\partial y}(\varphi p_t+\psi q_t) = 0, \quad \forall x,z, \tag{3.14}$$

$$\frac{\partial}{\partial t}E_3 + \frac{\partial}{\partial z}F_3 = \frac{\partial}{\partial t}(\zeta^2+\eta^2) - 2\frac{\partial}{\partial z}(\zeta p_t+\eta q_t) = 0, \quad \forall x,y, \tag{3.15}$$

$$\frac{d}{dt}[2V(x,y,z)(p^2+q^2) + \beta(p^2+q^2)^2] = 0, \qquad \forall x,y,z,t, \tag{3.16}$$

respectively. Moreover, for the nonlinear Hamiltonian system (3.6), one has the point-wise mass conservation law

$$|u(x,y,z,t)|^2 = |u(x,y,z,0)|^2, \quad \forall x,y,z,t, \tag{3.17}$$

which makes the subproblem exactly solvable by the method of separating variables.

4 LOD-MS for the GP equation

We can approximate the LOD MHPDEs (3.3)-(3.5) by some pairs of symplectic RK methods. This type of methods will make them satisfy discrete LOD MCLs [15].

We approximate the LOD MHPDEs (3.3), (3.4), (3.5) by the midpoint rule (2.12) and have

$$\begin{cases} -\dfrac{q^*_{\frac{1}{2},0,0}-q^n_{\frac{1}{2},0,0}}{\tau} + \dfrac{1}{2}\dfrac{v^{n*+\frac{1}{2}}_{1,0,0}-v^{n*+\frac{1}{2}}_{0,0,0}}{h} = 0, \\[2mm] \dfrac{p^*_{\frac{1}{2},0,0}-p^n_{\frac{1}{2},0,0}}{\tau} + \dfrac{1}{2}\dfrac{w^{n*+\frac{1}{2}}_{1,0,0}-w^{n*+\frac{1}{2}}_{0,0,0}}{h} = 0, \\[2mm] \dfrac{p^{n*+\frac{1}{2}}_{1,0,0}-p^{n*+\frac{1}{2}}_{0,0,0}}{h} = v^{n*+\frac{1}{2}}_{\frac{1}{2},0,0}, \qquad \dfrac{q^{n*+\frac{1}{2}}_{1,0,0}-q^{n*+\frac{1}{2}}_{0,0,0}}{h} = w^{n*+\frac{1}{2}}_{\frac{1}{2},0,0}, \end{cases} \tag{4.1}$$

$$\begin{cases} -\dfrac{q^{**}_{0,\frac{1}{2},0}-q^*_{0,\frac{1}{2},0}}{\tau} + \dfrac{1}{2}\dfrac{\varphi^{n**+\frac{1}{2}}_{0,1,0}-\varphi^{n**+\frac{1}{2}}_{0,0,0}}{h} = 0, \\[2mm] \dfrac{p^{**}_{0,\frac{1}{2},0}-p^*_{0,\frac{1}{2},0}}{\tau} + \dfrac{1}{2}\dfrac{\psi^{n**+\frac{1}{2}}_{0,1,0}-\psi^{n**+\frac{1}{2}}_{0,0,0}}{h} = 0, \\[2mm] \dfrac{p^{n**+\frac{1}{2}}_{0,1,0}-p^{n**+\frac{1}{2}}_{0,0,0}}{h} = \varphi^{n**+\frac{1}{2}}_{0,\frac{1}{2},0}, \qquad \dfrac{q^{n**+\frac{1}{2}}_{0,1,0}-q^{n**+\frac{1}{2}}_{0,0,0}}{h} = \psi^{n**+\frac{1}{2}}_{0,\frac{1}{2},0}, \end{cases} \tag{4.2}$$

$$\begin{cases} -\dfrac{q^{***}_{0,0,\frac{1}{2}}-q^{**}_{0,0,\frac{1}{2}}}{\tau} + \dfrac{1}{2}\dfrac{\zeta^{n***+\frac{1}{2}}_{0,0,1}-\zeta^{n***+\frac{1}{2}}_{0,0,0}}{h} = 0, \\[2mm] \dfrac{p^{***}_{0,0,\frac{1}{2}}-p^{**}_{0,0,\frac{1}{2}}}{\tau} + \dfrac{1}{2}\dfrac{\eta^{n***+\frac{1}{2}}_{0,0,1}-\eta^{n***+\frac{1}{2}}_{0,0,0}}{h} = 0, \\[2mm] \dfrac{p^{n***+\frac{1}{2}}_{0,0,1}-p^{n***+\frac{1}{2}}_{0,0,0}}{h} = \zeta^{n***+\frac{1}{2}}_{0,0,\frac{1}{2}}, \qquad \dfrac{q^{n***+\frac{1}{2}}_{0,0,1}-q^{n***+\frac{1}{2}}_{0,0,0}}{h} = \eta^{n***+\frac{1}{2}}_{0,0,\frac{1}{2}}, \end{cases} \tag{4.3}$$

where $u^{n*+\frac{1}{2}}=\frac{1}{2}(u^n+u^*)$, $u^{n**+\frac{1}{2}}=\frac{1}{2}(u^*+u^{**})$, $u^{n***+\frac{1}{2}}=\frac{1}{2}(u^{**}+u^{***})$. Here we have neglected the spatial indexes j,k,l.

As usual, the LOD-MS (4.1), (4.2), (4.3) can be coded in the following manner, respectively, by eliminating the conjugate momenta

$$i\frac{(u^*_{j-\frac{1}{2},kl}+u^*_{j+\frac{1}{2},kl})-(u^n_{j-\frac{1}{2},kl}+u^n_{j+\frac{1}{2},kl})}{\tau}+\delta_x^2 u^{n*+\frac{1}{2}}_{jkl}=0, \tag{4.4}$$

$$i\frac{(u^{**}_{j,k-\frac{1}{2},l}+u^{**}_{j,k+\frac{1}{2},l})-(u^*_{j,k-\frac{1}{2},l}+u^*_{j,k+\frac{1}{2},l})}{\tau}+\delta_y^2 u^{n**+\frac{1}{2}}_{jkl}=0, \tag{4.5}$$

$$i\frac{(u^{***}_{jk,l-\frac{1}{2}}+u^{***}_{jk,l+\frac{1}{2}})-(u^{**}_{jk,l-\frac{1}{2}}+u^{**}_{jk,l+\frac{1}{2}})}{\tau}+\delta_z^2 u^{n+\frac{1}{2}}_{jkl}=0, \tag{4.6}$$

where

$$\delta_x^2 u^n_{jkl}=\frac{u^n_{j+1,kl}-2u^n_{jkl}+u^n_{j-1,kl}}{h^2}, \qquad \delta_y^2 u^n_{jkl}=\frac{u^n_{j,k+1,l}-2u^n_{jkl}+u^n_{j,k-1,l}}{h^2},$$

$$\delta_z^2 u^n_{jkl}=\frac{u^n_{jk,l+1}-2u^n_{jkl}+u^n_{jk,l-1}}{h^2}.$$

As for the solver of Hamiltonian system (3.6), it can be exactly solved due to the point-wise conservation law (3.17)

$$u^{n+1}_{jkl}=\exp\left(-i(V_{jkl}+\beta|u^{***}_{jkl}|^2)\tau\right)u^{***}_{jkl}=\exp\left(-i\theta^{***}_{jkl}\right)u^{***}_{jkl}, \tag{4.7}$$

where $\theta^{***}_{jkl}=(V_{jkl}+\beta|u^{***}_{jkl}|^2)\tau$.

It can be observed that the scheme (4.4)-(4.7) is the first-order version (2.5). The discrete errors of the scheme (4.4)-(4.6) are of second-order accuracy in both time and space. The solution (4.7) is accurate. Therefore, the whole errors of the scheme (4.4)-(4.7) is of first-order in time and second-order in space. To improve the accuracy in time, we composite schemes (4.4)-(4.7) by using the second-order version (2.6) and obtain

$$i\frac{(u^*_{j-\frac{1}{2},kl}+u^*_{j+\frac{1}{2},kl})-(u^n_{j-\frac{1}{2},kl}+u^n_{j+\frac{1}{2},kl})}{\tau/2}+\delta_x^2 u^{n*+\frac{1}{2}}_{jkl}=0, \tag{4.8}$$

$$i\frac{(u^{**}_{j,k-\frac{1}{2},l}+u^{**}_{j,k+\frac{1}{2},l})-(u^*_{j,k-\frac{1}{2},l}+u^*_{j,k+\frac{1}{2},l})}{\tau/2}+\delta_y^2 u^{n**+\frac{1}{2}}_{jkl}=0, \tag{4.9}$$

$$i\frac{(u^{***}_{jk,l-\frac{1}{2}}+u^{***}_{jk,l+\frac{1}{2}})-(u^{**}_{jk,l-\frac{1}{2}}+u^{**}_{jk,l+\frac{1}{2}})}{\tau/2}+\delta_z^2 u^{n+\frac{1}{2}}_{jkl}=0, \tag{4.10}$$

$$\bar{u}_{jkl}=\exp\left(-i(V_{jkl}+\beta|u^{***}_{jkl}|^2)\tau\right)u^{***}_{jkl}=\exp\left(-i\theta^{***}_{jkl}\right)u^{***}_{jkl}, \tag{4.11}$$

$$i\frac{(\bar{\bar{u}}_{jk,l-\frac{1}{2}}+\bar{\bar{u}}_{jk,l+\frac{1}{2}})-(\bar{u}_{jk,l-\frac{1}{2}}+\bar{u}_{jk,l+\frac{1}{2}})}{\tau/2}+\delta_z^2 u_{jkl}^{n\diamond+\frac{1}{2}}=0, \tag{4.12}$$

$$i\frac{(\bar{\bar{\bar{u}}}_{j,k-\frac{1}{2},l}+\bar{\bar{\bar{u}}}_{j,k+\frac{1}{2},l})-(\bar{\bar{u}}_{j,k-\frac{1}{2},l}+\bar{\bar{u}}_{j,k+\frac{1}{2},l})}{\tau/2}+\delta_y^2 u_{jkl}^{n\diamond\diamond+\frac{1}{2}}=0, \tag{4.13}$$

$$i\frac{(u_{j-\frac{1}{2},kl}^{n+1}+u_{j+\frac{1}{2},kl}^{n+1})-(\bar{\bar{\bar{u}}}_{j-\frac{1}{2},kl}+\bar{\bar{\bar{u}}}_{j+\frac{1}{2},kl})}{\tau/2}+\delta_x^2 u_{jkl}^{n\diamond\diamond\diamond+\frac{1}{2}}=0. \tag{4.14}$$

where $u^{n\diamond+\frac{1}{2}}=\frac{1}{2}(\bar{u}+\bar{\bar{u}})$, $u^{n\diamond\diamond+\frac{1}{2}}=\frac{1}{2}(\bar{\bar{u}}+\bar{\bar{\bar{u}}})$, $u^{n\diamond\diamond\diamond+\frac{1}{2}}=\frac{1}{2}(\bar{\bar{\bar{u}}}+u^{n+1})$. For simplicity, we denote LOD-MS (4.4)-(4.7) as LOD-MS I and LOD-MS (4.8)-(4.14) as LOD-MS II.

5   Analysis of conservative properties

In this section, we investigate the LOD-MS I theoretically. The numerical analysis of the second-order scheme LOD-MS II can be programmed in the same way. For convenience, the unitary inner product and l_2-norm are recalled:

$$\langle u,v\rangle=h_x h_y h_z\sum_{j,k,l}u_{jkl}\bar{v}_{jkl}, \qquad \|u\|^2=\langle u,u\rangle,$$

$$\|u\|_{\frac{1}{2}}^2=h_x h_y h_z\sum_{j,k,l}|u_{j+\frac{1}{2},k+\frac{1}{2},l+\frac{1}{2}}|^2, \quad \|u\|_\infty=\max_{j,k,l}|u_{jkl}|.$$

By the theory in multisymplectic background, the LOD schemes (4.1), (4.2), (4.3) satisfy the discrete LOD MCLs

$$\frac{\omega_{j+\frac{1}{2},kl}^*-\omega_{j+\frac{1}{2},kl}^n}{\tau}+\frac{\kappa_{1\,j+1,kl}^{n*+\frac{1}{2}}-\kappa_{1\,jkl}^{n*+\frac{1}{2}}}{h}=0, \tag{5.1}$$

$$\frac{\omega_{j,k+\frac{1}{2},l}^{**}-\omega_{j,k+\frac{1}{2},l}^*}{\tau}+\frac{\kappa_{2\,j,k+1,l}^{n**+\frac{1}{2}}-\kappa_{2\,jkl}^{n**+\frac{1}{2}}}{h}=0, \tag{5.2}$$

$$\frac{\omega_{jk,l+\frac{1}{2}}^{***}-\omega_{jk,l+\frac{1}{2}}^{**}}{\tau}+\frac{\kappa_{3\,jk,l+1}^{n***+\frac{1}{2}}-\kappa_{3\,jkl}^{n***+\frac{1}{2}}}{h}=0, \tag{5.3}$$

and the LOD LECLs

$$\frac{E_{1\,j+\frac{1}{2},kl}^*-E_{1\,j+\frac{1}{2},kl}^n}{\tau}+\frac{F_{1\,j+1,kl}^{n*+\frac{1}{2}}-F_{1\,jkl}^{n*+\frac{1}{2}}}{h}=0, \tag{5.4}$$

$$\frac{E_{2\,j,k+\frac{1}{2},l}^{**}-E_{2\,j,k+\frac{1}{2},l}^*}{\tau}+\frac{F_{2\,j,k+1,l}^{n**+\frac{1}{2}}-F_{2\,jkl}^{n**+\frac{1}{2}}}{h}=0, \tag{5.5}$$

$$\frac{E_{3\,jk,l+\frac{1}{2}}^{***}-E_{3\,jk,l+\frac{1}{2}}^{**}}{\tau}+\frac{F_{3\,jk,l+1}^{n***+\frac{1}{2}}-F_{3\,jkl}^{n***+\frac{1}{2}}}{h}=0, \tag{5.6}$$

where

$$E1^n_{j+\frac{1}{2},kl} = (v^n_{j+\frac{1}{2},kl})^2 + (w^n_{j+\frac{1}{2},kl})^2,$$

$$E2^*_{j,k+\frac{1}{2},l} = (\varphi^*_{j,k+\frac{1}{2},l})^2 + (\psi^*_{j,k+\frac{1}{2},l})^2,$$

$$E3^{**}_{jk,l+\frac{1}{2}} = (\zeta^{**}_{jk,l+\frac{1}{2}})^2 + (\eta^{**}_{jk,l+\frac{1}{2}})^2,$$

$$F1^{n*+\frac{1}{2}}_{jkl} = -2(v^{n*+\frac{1}{2}}_{jkl}\delta_t p^{n*+\frac{1}{2}}_{jkl} + w^{n*+\frac{1}{2}}_{jkl}\delta_t q^{n*+\frac{1}{2}}_{jkl}),$$

$$F2^{n**+\frac{1}{2}}_{jkl} = -2(\varphi^{n**+\frac{1}{2}}_{jkl}\delta_t p^{n**+\frac{1}{2}}_{jkl} + \psi^{n**+\frac{1}{2}}_{jkl}\delta_t q^{n**+\frac{1}{2}}_{jkl}),$$

$$F3^{n***+\frac{1}{2}}_{jkl} = -2(\zeta^{n***+\frac{1}{2}}_{jkl}\delta_t p^{n***+\frac{1}{2}}_{jkl} + \eta^{n***+\frac{1}{2}}_{jkl}\delta_t q^{n***+\frac{1}{2}}_{jkl}).$$

Of course, the solution (4.7) of the nonlinear subproblem (3.6) satisfies the conservation laws that the original system (3.6) possesses, such as symplectic-preserving, point-wise mass-preserving and point-wise energy-preserving as well

$$dq^{n+1}_{jkl} \wedge dp^{n+1}_{jkl} = dq^n_{jkl} \wedge dp^n_{jkl} = \cdots = dq^0_{jkl} \wedge dp^0_{jkl}, \tag{5.7}$$

$$|u^{n+1}_{jkl}|^2 = |u^n_{jkl}|^2 = \cdots = |u^0_{jkl}|^2, \tag{5.8}$$

$$2V_{jkl}|u^{n+1}_{jkl}|^2 + \beta|u^{n+1}_{jkl}|^4 = 2V_{jkl}|u^n_{jkl}|^2 + \beta|u^n_{jkl}|^4 = \cdots = 2V_{jkl}|u^0_{jkl}|^2 + \beta|u^0_{jkl}|^4. \tag{5.9}$$

In fact, the solution (4.7) can be written in

$$p^{n+1}_{jkl} + iq^{n+1}_{jkl} = \left(\cos\theta^n_{jkl} - i\sin\theta^n_{jkl}\right)(p^n_{jkl} + iq^n_{jkl}).$$

That is to say,

$$\begin{cases} p^{n+1}_{jkl} = p^n_{jkl}\cos\theta^n_{jkl} + q^n_{jkl}\sin\theta^n_{jkl}, \\ q^{n+1}_{jkl} = -p^n_{jkl}\sin\theta^n_{jkl} + q^n_{jkl}\cos\theta^n_{jkl}. \end{cases}$$

Consequently, one has

$$dq^{n+1}_{jkl} \wedge dp^{n+1}_{jkl} = \left[-dp^n_{jkl}\sin\theta^n_{jkl} + dq^n_{jkl}\cos\theta^n_{jkl}\right] \wedge \left[dp^n_{jkl}\cos\theta^n_{jkl} + dq^n_{jkl}\sin\theta^n_{jkl}\right]$$
$$= dq^n_{jkl} \wedge dp^n_{jkl}.$$

This is precisely the symplectic conservation law (5.7). Taking the norm on both sides of (4.7), it results in the point-wise mass invariant (5.8). The third invariant (5.9) can be derived from the second one (5.8).

To pick up the total conservation laws of the LOD-MS (4.1), (4.2), (4.3) and (4.7), we

reformulate them into follows:

$$
\begin{cases}
\dfrac{q^*_{j+\frac{1}{2},k+\frac{1}{2},l+\frac{1}{2}}-q^n_{j+\frac{1}{2},k+\frac{1}{2},l+\frac{1}{2}}}{\tau}-\dfrac{1}{2}\dfrac{v^{n*+\frac{1}{2}}_{j+1,k+\frac{1}{2},l+\frac{1}{2}}-v^{n*+\frac{1}{2}}_{j,k+\frac{1}{2},l+\frac{1}{2}}}{h}=0,\\[3mm]
-\dfrac{p^*_{j+\frac{1}{2},k+\frac{1}{2},l+\frac{1}{2}}-p^n_{j+\frac{1}{2},k+\frac{1}{2},l+\frac{1}{2}}}{\tau}-\dfrac{1}{2}\dfrac{w^{n*+\frac{1}{2}}_{j+1,k+\frac{1}{2},l+\frac{1}{2}}-w^{n*+\frac{1}{2}}_{j,k+\frac{1}{2},l+\frac{1}{2}}}{h}=0,\\[3mm]
\dfrac{1}{2}\dfrac{p^{n*+\frac{1}{2}}_{j+1,k+\frac{1}{2},l+\frac{1}{2}}-p^{n*+\frac{1}{2}}_{j,k+\frac{1}{2},l+\frac{1}{2}}}{h}=\dfrac{1}{2}v^{n*+\frac{1}{2}}_{j+\frac{1}{2},j+\frac{1}{2},l+\frac{1}{2}},\\[3mm]
\dfrac{1}{2}\dfrac{q^{n*+\frac{1}{2}}_{j+1,k+\frac{1}{2},l+\frac{1}{2}}-q^{n*+\frac{1}{2}}_{j,k+\frac{1}{2},l+\frac{1}{2}}}{h}=\dfrac{1}{2}w^{n*+\frac{1}{2}}_{j+\frac{1}{2},k+\frac{1}{2},l+\frac{1}{2}},
\end{cases}
\tag{5.10}
$$

$$
\begin{cases}
\dfrac{q^{**}_{j+\frac{1}{2},k+\frac{1}{2},l+\frac{1}{2}}-q^*_{j+\frac{1}{2},k+\frac{1}{2},l+\frac{1}{2}}}{\tau}-\dfrac{1}{2}\dfrac{\varphi^{n**+\frac{1}{2}}_{j+\frac{1}{2},k+1,l+\frac{1}{2}}-\varphi^{n**+\frac{1}{2}}_{j+\frac{1}{2},k,l+\frac{1}{2}}}{h}=0,\\[3mm]
-\dfrac{p^{**}_{j+\frac{1}{2},k+\frac{1}{2},l+\frac{1}{2}}-p^*_{j+\frac{1}{2},k+\frac{1}{2},l+\frac{1}{2}}}{\tau}-\dfrac{1}{2}\dfrac{\psi^{n+\frac{1}{2}}_{j+\frac{1}{2},k+1,l+\frac{1}{2}}-\psi^{n+*+\frac{1}{2}}_{j+\frac{1}{2},k,l+\frac{1}{2}}}{h}=0,\\[3mm]
\dfrac{1}{2}\dfrac{p^{n**+\frac{1}{2}}_{j+\frac{1}{2},k+1,l+\frac{1}{2}}-p^{n**+\frac{1}{2}}_{j+\frac{1}{2},k,l+\frac{1}{2}}}{h}=\dfrac{1}{2}\varphi^{n**+\frac{1}{2}}_{j+\frac{1}{2},k+\frac{1}{2},l+\frac{1}{2}},\\[3mm]
\dfrac{1}{2}\dfrac{q^{n**+\frac{1}{2}}_{j+\frac{1}{2},k+1,l+\frac{1}{2}}-q^{n**+\frac{1}{2}}_{j+\frac{1}{2},k,l+\frac{1}{2}}}{h}=\dfrac{1}{2}\psi^{n**+\frac{1}{2}}_{j+\frac{1}{2},k+\frac{1}{2},l+\frac{1}{2}},
\end{cases}
\tag{5.11}
$$

$$
\begin{cases}
\dfrac{q^{***}_{j+\frac{1}{2},k+\frac{1}{2},l+\frac{1}{2}}-q^{**}_{j+\frac{1}{2},k+\frac{1}{2},l+\frac{1}{2}}}{\tau}-\dfrac{1}{2}\dfrac{\zeta^{n***+\frac{1}{2}}_{j+\frac{1}{2},k+\frac{1}{2},l+1}-\zeta^{n***+\frac{1}{2}}_{j+\frac{1}{2},k+\frac{1}{2},l}}{h}=0,\\[3mm]
-\dfrac{p^{***}_{j+\frac{1}{2},k+\frac{1}{2},l+\frac{1}{2}}-p^{**}_{j+\frac{1}{2},k+\frac{1}{2},l+\frac{1}{2}}}{\tau}-\dfrac{1}{2}\dfrac{\eta^{n***+\frac{1}{2}}_{j+\frac{1}{2},k+\frac{1}{2},l+1}-\eta^{n***+\frac{1}{2}}_{j+\frac{1}{2},k+\frac{1}{2},l}}{h}=0,\\[3mm]
\dfrac{1}{2}\dfrac{p^{n***+\frac{1}{2}}_{j+\frac{1}{2},k+\frac{1}{2},l+1}-p^{n***+\frac{1}{2}}_{j+\frac{1}{2},k+\frac{1}{2},l}}{h}=\dfrac{1}{2}\zeta^{n***+\frac{1}{2}}_{j+\frac{1}{2},k+\frac{1}{2},l+\frac{1}{2}},\\[3mm]
\dfrac{1}{2}\dfrac{q^{n***+\frac{1}{2}}_{j+\frac{1}{2},k+\frac{1}{2},l+1}-q^{n***+\frac{1}{2}}_{j+\frac{1}{2},k+\frac{1}{2},l}}{h}=\dfrac{1}{2}\eta^{n***+\frac{1}{2}}_{j+\frac{1}{2},k+\frac{1}{2},l+\frac{1}{2}},
\end{cases}
\tag{5.12}
$$

$$
u^{n+1}_{\frac{1}{2},\frac{1}{2},\frac{1}{2}}=\exp\left(-i(V_{\frac{1}{2},\frac{1}{2},\frac{1}{2}}+\beta|u^{***}_{\frac{1}{2},\frac{1}{2},\frac{1}{2}}|^2)\tau\right)u^{***}_{\frac{1}{2},\frac{1}{2},\frac{1}{2}}=\exp\left(-i\theta^{***}_{\frac{1}{2},\frac{1}{2},\frac{1}{2}}\right)u^{***}_{\frac{1}{2},\frac{1}{2},\frac{1}{2}}.
\tag{5.13}
$$

As a counterpart of (4.4), (4.5), (4.6), the schemes (5.10), (5.11), (5.12), (5.13) can be coded as follows:

$$
i\delta_t(u^{n*+\frac{1}{2}}_{j+\frac{1}{2},k+\frac{1}{2},l+\frac{1}{2}}+u^{n*+\frac{1}{2}}_{j-\frac{1}{2},k+\frac{1}{2},l+\frac{1}{2}})+\delta_x^2 u^{n*+\frac{1}{2}}_{j,k+\frac{1}{2},l+\frac{1}{2}}=0,
\tag{5.14}
$$

$$
i\delta_t(u^{n**+\frac{1}{2}}_{j+\frac{1}{2},k+\frac{1}{2},l+\frac{1}{2}}+u^{n**+\frac{1}{2}}_{j+\frac{1}{2},k-\frac{1}{2},l+\frac{1}{2}})+\delta_y^2 u^{n**+\frac{1}{2}}_{j+\frac{1}{2},k,l+\frac{1}{2}}=0,
\tag{5.15}
$$

$$i\delta_t\big(u^{n****+\frac{1}{2}}_{j+\frac{1}{2},k+\frac{1}{2},l+\frac{1}{2}}+u^{n****+\frac{1}{2}}_{j+\frac{1}{2},k+\frac{1}{2},l-\frac{1}{2}}\big)+\delta_z^2 u^{n****+\frac{1}{2}}_{j+\frac{1}{2},k+\frac{1}{2},l}=0,\tag{5.16}$$

$$u^{n+1}_{\frac{1}{2},\frac{1}{2},\frac{1}{2}}=\exp\Big(-i(V_{\frac{1}{2},\frac{1}{2},\frac{1}{2}}+\beta|u^{***}_{\frac{1}{2},\frac{1}{2},\frac{1}{2}}|^2)\tau\Big)u^{***}_{\frac{1}{2},\frac{1}{2},\frac{1}{2}}=\exp\Big(-i\theta^{***}_{\frac{1}{2},\frac{1}{2},\frac{1}{2}}\Big)u^{***}_{\frac{1}{2},\frac{1}{2},\frac{1}{2}}.\tag{5.17}$$

Theorem 5.1. *The LOD-MS (4.4)-(4.7) admits the global mass and global LOD energy conservation laws*

$$\mathcal{Q}^{n+1}=\mathcal{Q}^{***}=\mathcal{Q}^{**}=\mathcal{Q}^{*}=\mathcal{Q}^{n}=\cdots=\mathcal{Q}^{0},\tag{5.18}$$

$$\mathcal{E}_x^*=\mathcal{E}_x^n,\quad \mathcal{E}_y^{**}=\mathcal{E}_y^*,\quad \mathcal{E}_z^{***}=\mathcal{E}_z^{**},\tag{5.19}$$

where

$$\mathcal{Q}=\|u\|_{\frac{1}{2}}^2,\qquad\qquad \mathcal{E}_x=h_x h_y h_z\sum_{j,k,l}|\delta_x u_{j+\frac{1}{2},k,l}|^2,$$

$$\mathcal{E}_y=h_x h_y h_z\sum_{j,k,l}|\delta_y u_{j,k+\frac{1}{2},l}|^2,\quad \mathcal{E}_z=h_x h_y h_z\sum_{j,k,l}|\delta_z u_{j,k,l+\frac{1}{2}}|^2,$$

with the centered difference quotient $\delta_s u_{m+\frac{1}{2}}=\frac{u_{m+1}-u_m}{h_s}$.

Remark 5.1. From the point-wise conservation laws (5.8), (5.9), it is quite clear that

$$\mathcal{Q}^{n+1}=\mathcal{Q}^{****}=\mathcal{Q}^{n},\tag{5.20}$$

$$\mathcal{E}_{non}^{n+1}=h^3\sum_{j,k,l}\Big[V_{jkl}|u^{n+1}_{jkl}|^2+\beta|u^{n+1}_{jkl}|^4\Big]=\mathcal{E}^{***}_{non}.\tag{5.21}$$

Therefore, the proposed LOD-MS (4.4)-(4.7) is unconditionally stable.

In what follows, we investigate the energy conservation laws of the novel LOD-MS (4.1), (4.2), (4.3) and (4.7), including LECL and global energy conservation law.

Theorem 5.2. *Let the solution function $u(x,y,z,t)$ of the GP equation (1.2) be variable separable, i.e.,*

$$u(x,y,z,t)=X(x)Y(y)Z(z)T(t),\tag{5.22}$$

or equally

$$u^n_{jkl}=T^n X_j Y_k Z_l.\tag{5.23}$$

Then the LOD-MS (4.1)-(4.3), and (4.7) is local energy conservative

$$\frac{E^{n+1}_{j+\frac{1}{2},k+\frac{1}{2},l+\frac{1}{2}}-E^n_{j+\frac{1}{2},k+\frac{1}{2},l+\frac{1}{2}}}{\tau}+\nabla_h\cdot\mathbf{F}^{n+\frac{1}{2}}_{jkl}=0.\tag{5.24}$$

Proof. Under the assumption of (5.23) and the discrete mass conservation law (5.20), one has

$$|T^{n+1}|^2 = |T^{***}|^2 = |T^{**}|^2 = |T^*|^2 = |T^n|^2 = \cdots = |T^0|^2, \tag{5.25}$$

and

$$\delta_t u_{jkl}^{n+\frac{1}{2}} = (\delta_t T^{n+\frac{1}{2}})X_j Y_k Z_l, \qquad \delta_x u_{j+\frac{1}{2},kl}^{n+\frac{1}{2}} = T^{n+\frac{1}{2}}(\delta_x X_{j+\frac{1}{2}})Y_k Z_l,$$

$$\delta_y u_{j,k+\frac{1}{2},l}^{n+\frac{1}{2}} = T^{n+\frac{1}{2}} X_j (\delta_y Y_{k+\frac{1}{2}})Z_l, \quad \delta_z u_{jk,l+\frac{1}{2}}^{n+\frac{1}{2}} = (T^{n+\frac{1}{2}} X_j Y_k \delta_z Z_{l+\frac{1}{2}}).$$

It is reasonable to form a hypothesis as follows:

$$p_{jkl}^n = T_p^n X_{p_j} Y_{p_k} Z_{p_l}, \qquad q_{jkl}^n = T_q^n X_{p_j} Y_{q_k} Z_{q_l},$$

$$v_{jkl}^n = T_p^n \delta_x X_{p_j} Y_{p_k} Z_{p_l}, \quad w_{jkl}^n = T_q^n \delta_x X_{q_j} Y_{q_k} Z_{q_l},$$

$$\varphi_{jkl}^n = T_p^n X_{p_j} \delta_y Y_{p_k} Z_{p_l}, \quad \psi_{jkl}^n = T_q^n X_{q_j} \delta_y Y_{q_k} Z_{q_l},$$

$$\zeta_{jkl}^n = T_p^n X_{p_j} Y_{p_k} \delta_z Z_{p_l}, \quad \eta_{jkl}^n = T_q^n X_{q_j} Y_{q_k} \delta_z Z_{q_l},$$

then

$$|T^n|^2 = (T_p^n)^2 + (T_q^n)^2. \tag{5.26}$$

Thus, it is reminding (5.25) that the three LOD LECLs (5.4), (5.5) and (5.6) can be replaced by

$$\frac{E1_{j+\frac{1}{2},kl}^{n+1} - E1_{j+\frac{1}{2},kl}^n}{\tau} + \frac{F1_{j+1,kl}^{n*+\frac{1}{2}} - F1_{jkl}^{n+\frac{1}{2}}}{h} = 0, \tag{5.27}$$

$$\frac{E2_{j,k+\frac{1}{2},l}^{n+1} - E2_{j,k+\frac{1}{2},l}^n}{\tau} + \frac{F2_{j,k+1,l}^{n+\frac{1}{2}} - F2_{jkl}^{n+\frac{1}{2}}}{h} = 0, \tag{5.28}$$

$$\frac{E3_{jk,l+\frac{1}{2}}^{n+1} - E3_{jk,l+\frac{1}{2}}^n}{\tau} + \frac{F3_{jk,l+1}^{n+\frac{1}{2}} - F3_{jkl}^{n+\frac{1}{2}}}{h} = 0. \tag{5.29}$$

Adding up the above three equalities and (5.9), we obtain the discrete LECL (5.24). This proof is finished. □

Theorem 5.3. *The LOD-MS I and LOD-MS II conserves the discrete energy exactly*

$$\mathcal{E}^{n+1} = \mathcal{E}^n = \cdots = \mathcal{E}^0, \tag{5.30}$$

where

$$\mathcal{E}^n = h^3 \sum_{j,k,l} \left[(2V_{jkl} + |u_{jkl}^n|^2)|u_{jkl}^n|^2 + |\nabla_h u_{jkl}^n|^2 \right],$$

with the discrete gradient $\nabla_h u_{jkl}^n = |\delta_x u_{j+\frac{1}{2},kl}^n|^2 + |\delta_y u_{jk+\frac{1}{2},l}^n|^2 + |\delta_z u_{jk,l+\frac{1}{2}}^n|^2$, *provided that the solution is separable in terms of the independent variables.*

Proof. Using (5.23), (5.9) and (5.25), the global LOD energy conservation laws (5.19) and (5.21) can be written as

$$|T^{n+1}|^2 \sum_{j,k,l} |Y_k Z_l \delta_x X_{j+\frac{1}{2}}|^2 = |T^n|^2 \sum_{j,k,l} |Y_k Z_l \delta_x X_{j+\frac{1}{2}}|^2, \tag{5.31}$$

$$|T^{n+1}|^2 \sum_{j,k,l} |X_j Z_l \delta_y Y_{k+\frac{1}{2}}|^2 = |T^n|^2 \sum_{j,k,l} |X_j Z_l \delta_y Y_{k+\frac{1}{2}}|^2, \tag{5.32}$$

$$|T^{n+1}|^2 \sum_{j,k,l} |X_j Y_k \delta_z Z_{l+\frac{1}{2}}|^2 = |T^n|^2 \sum_{j,k,l} |X_j Y_k \delta_z Z_{l+\frac{1}{2}}|^2, \tag{5.33}$$

$$h^3 \sum_{j,k,l} \left(2V_{jkl} |u_{jkl}^{n+1}|^2 + \beta |u_{jkl}^{n+1}|^4 \right) = h^3 \sum_{j,k,l} \left(2V_{jkl} |u_{jkl}^n|^2 + \beta |u_{jkl}^n|^4 \right). \tag{5.34}$$

Sum over the above equalities, we get

$$
\begin{aligned}
&h^3 \sum_{j,k,l} (2V_{jkl} |u_{jkl}^{n+1}|^2 + \beta |u_{jkl}^{n+1}|^4) + \left\| \nabla_h u^{n+1} \right\|^2 \\
&= h^3 \sum_{j,k,l} (2V_{jkl} |u_{jkl}^n|^2 + \beta |u_{jkl}^n|^4) + \|\nabla_h u^n\|^2.
\end{aligned} \tag{5.35}
$$

This is just what we desire. The proof is finished. □

Remark 5.2. It is noted that the conclusions in Theorems 5.2 and 5.3 are true in case of the solution function is separable. Otherwise, they will not always necessarily true.

Remark 5.3. The LOD-MS for GP equations and the conclusions we have obtained can be extended to some initial boundary problem, such as, periodic boundary condition, Dirichlet boundary condition. This will be verified in the following numerical illustrations.

6 Numerical examples

In this section, we will take several examples to investigate the numerical behavior of the LOD-MS. We will observe that the developed scheme is economic and simply in coding. For convenience, we define the following notations to present numerical results.

$$e_2^n = h^3 \sqrt{\sum_{j,k,l} |u_{jkl}^n - \hat{u}_{jkl}^n|^2}, \quad e_\infty^n = \max_{j,k,l} |u_{jkl}^n - \hat{u}_{jkl}^n|,$$

where u_{jkl}^n and $\hat{u}_{jkl}^n$ denote approximate solution and exact solution, respectively.

Example 6.1. The test problem in 1d

$$
\begin{cases}
i\dfrac{\partial}{\partial t} u(x,t) = -\dfrac{1}{2} u_{xx} + V(x)u + |u|^2 u, \\
u(x,0) = \sin x,
\end{cases} \tag{6.1}
$$

where $V(x) = \cos^2 x$ is a periodic potential. The exact solution for the problem is

$$u(x,t) = e^{-3it/2} \sin x.$$

First, we test the convergence rate in the space direction. To the purpose, we fix the time step length very small, such as $\tau = 0.0001$, such that nearly all the discretization error comes from the space. The numerical errors and their convergence rates under different spatial steps at different time t are listed in Table 1, which implies that LOD-MS II is indeed of second-order accuracy in space. Here the convergence rate *order* is calculated by formula $order = \ln(e_{s_1}/e_{s_2})/\ln(s_1/s_2)$, where e_{s_m}, $m = 1,2$, are numerical errors using step length s_m.

Table 1: The errors and spatial accuracy at different time t.

t	h	e_∞^n	order	e_2^n	order
8	$\pi/20$	1.6507×10^{-2}	–	1.1596×10^{-2}	–
	$\pi/40$	4.1159×10^{-3}	2.0037	2.0445×10^{-3}	2.5038
16	$\pi/20$	3.3013×10^{-2}	–	2.3191×10^{-2}	–
	$\pi/40$	8.2318×10^{-3}	2.0038	4.0890×10^{-3}	2.5037
24	$\pi/20$	4.9516×10^{-2}	–	3.4784×10^{-2}	–
	$\pi/40$	1.2348×10^{-2}	2.0038	6.1335×10^{-3}	2.5036
32	$\pi/20$	6.6018×10^{-2}	–	4.6375×10^{-2}	–
	$\pi/40$	1.6464×10^{-2}	2.0036	8.1779×10^{-3}	2.5035

Next, we investigate the time convergence rate of the LOD-MS II via the above problem over $t \in [0,25]$. We take the spatial step length small enough so that error from spatial discretization is negligible, such as $h = \frac{\pi}{1000}$. Moreover, we compare its computational efficiency with the general MI for the problem

$$\frac{(u_{j-\frac{1}{2}}^{n+1} + u_{j+\frac{1}{2}}^{n+1}) - (u_{j-\frac{1}{2}}^n + u_{j+\frac{1}{2}}^n)}{\tau} + 2\delta_x^2 u_j^{n+\frac{1}{2}} - V_{j-\frac{1}{2}} u_{j-\frac{1}{2}}^{n+\frac{1}{2}} - V_{j+\frac{1}{2}} u_{j+\frac{1}{2}}^{n+\frac{1}{2}}$$

$$= \left| u_{j-\frac{1}{2}}^{n+\frac{1}{2}} \right|^2 u_{j-\frac{1}{2}}^{n+\frac{1}{2}} + \left| u_{j+\frac{1}{2}}^{n+\frac{1}{2}} \right|^2 u_{j+\frac{1}{2}}^{n+\frac{1}{2}}. \tag{6.2}$$

The time step lengths are $\tau = 0.025$, $\tau = 0.05$ and $\tau = 0.1$. We simulate the problem with both LOD-MS II and (6.2). Fig. 1 reports the numerical error and temporal convergence rate against time of LOD-MS II. Data in Table 2 show the computational efficiency of the

Table 2: The comparison of the efficiency of different schemes at $t = 100$.

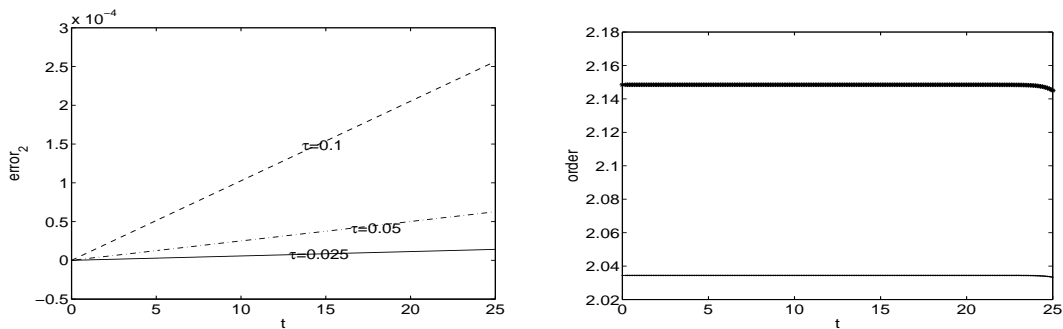| $\tau \backslash$ scheme	LOD-MS II			(6.2)		
	e_2	e_∞	CPU(sec)	e_2	e_∞	CPU(sec)
0.1	$5.31e-5$	$1.70e-1$	2.7	$2.46e-4$	$5.23e-3$	35
0.05	$1.34e-5$	$4.29e-2$	5.4	$6.27e-5$	$7.14e-4$	55
0.025	$3.36e-6$	$1.07e-2$	11	$1.42e-5$	$1.93e-4$	84

Figure 1: The time error and order test: left for error and right for order.

two methods. Numerical results indicate that the LOD-MS II is of second-order in time and is much more efficient than method (6.2).

We shall not compare the efficiency of LOD-MS with the completely implicit MI for multidimensional problems resembling (6.2) any more due to the performance restriction of personal computer.

Example 6.2. Next, we consider the following two-dimensional nonlinear initial-boundary value problem with a periodic potential

$$\begin{cases} i\dfrac{\partial u(x,y,t)}{\partial t} = -\dfrac{1}{2}(u_{xx}+u_{yy})+V(x,y)u+|u|^2u, \\ u(x,y,0)=\sin x\sin y, \quad (x,y)\in[0,2\pi]\times[0,2\pi], \end{cases} \tag{6.3}$$

with $V(x,y)=1-\sin^2 x\sin^2 y$. The exact solution of Eq. (6.3) is

$$u(x,y,t)=e^{-2it}\sin x\sin y.$$

We choose $\tau=0.02, h=\pi/20$ to investigate the performance of the LOD-MS II, including the conservative properties and wave shape. Fig. 2 presents the real part and imaginary part of the numerical solution at $t=50$. Fig. 3 shows the residuals of mass and global
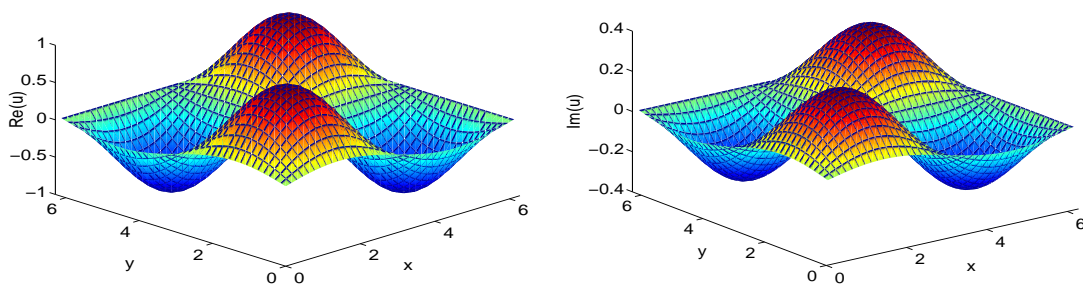
Figure 2: The numerical solutions, left for real part, right for imaginary part.
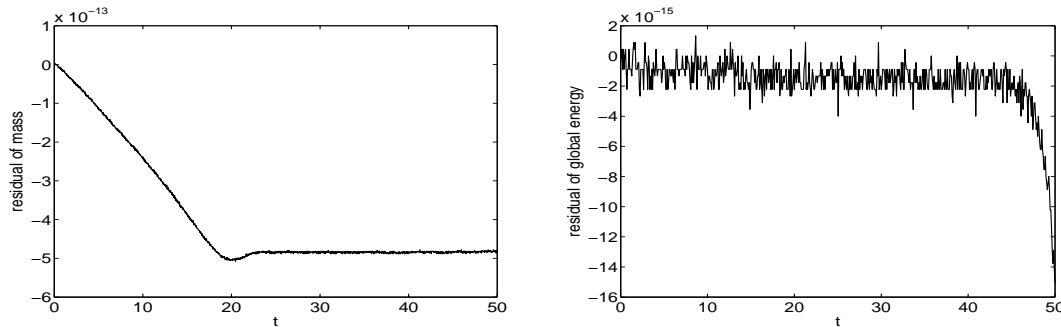
Figure 3: The residuals of mass and global energy, left for mass, right for global energy.

energy against time. From the figures, it is observed that the LOD-MS II can simulate the continuous problem very well over a long period, and it preserves the conservative quantities accurately.

Example 6.3. In the example, we consider a 3D problem with exact solution to check the theoretical analysis and to illustrate the capability of LOD-MS II in simulating 3D problems. The periodic problem is

$$
\begin{cases}
i\dfrac{\partial u}{\partial t} = -\dfrac{1}{2}(u_{xx}+u_{yy}+u_{zz})+V(x,y,z)u+|u|^2u, \\
u(x,y,0) = \sin x \sin y \sin z, \quad (x,y,z)\in[0,2\pi]^3,
\end{cases}
\tag{6.4}
$$

where $V(x,y,z)=1-\sin^2 x\sin^2 y\sin^2 z$ is a periodic potential. The exact solution of the problem is

$$
u(x,y,z,t)=e^{-5it/2}\sin x\sin y\sin z,
$$

which is variable separable. In the case, the Theorems 5.1 and 5.2 are valid.

We choose $\tau=0.01, h=\frac{2\pi}{25}$ to execute the experiment with LOD-MS II, and focus on the numerical error e_2^n of the wave function and the conservation laws. Fig. 4 presents the former and the residual of mass against time, and Fig. 5 shows the residuals of global and local energy conservation laws against time. As the results of Theorems 5.1 and 5.2 is predicted, the LOD-MS II preserves the mass, global energy and local energy exactly in that their residuals are within the roundoff error.

Example 6.4. In the example, we investigate the 3d anisotropic condensate problem with changing trapped frequency

$$
\begin{cases}
i\psi_t = -\dfrac{1}{2}\nabla^2 u+V(x,y,z)u+\dfrac{1}{10}|\psi|^2\psi, \\
\psi(x,y,z,0) = \dfrac{2^{1/4}}{(\pi/4)^{3/8}}\exp(-2(x^2+2y^2+4z^2)),
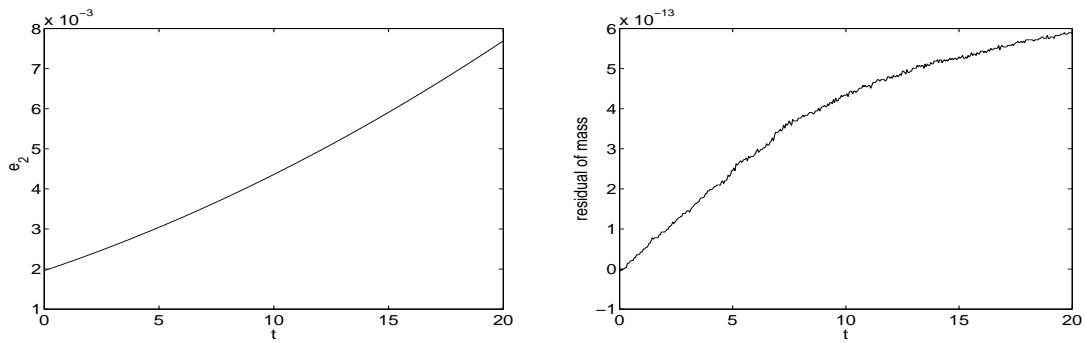\end{cases}
\tag{6.5}
$$

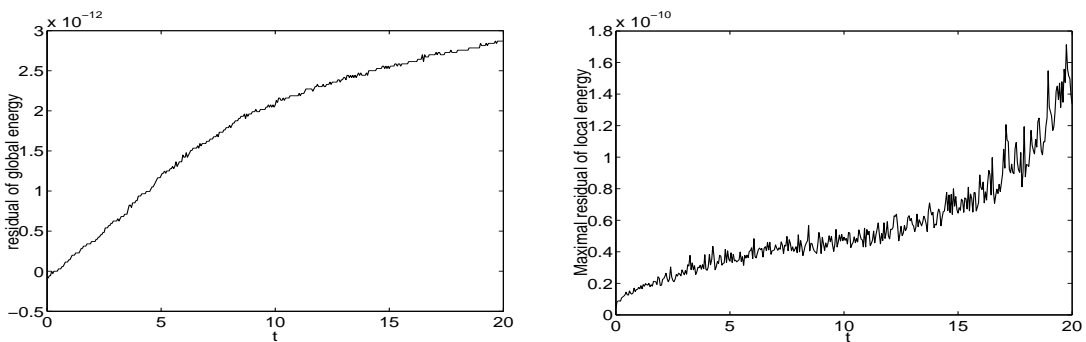Figure 4: The numerical error of wave function and residual of mass. Left for numerical error; Right for residual of mass.

Figure 5: The residuals of global and local energy, left for global, right for local.

where $V_3(x,y,z) = \frac{1}{2}(x^2+4y^2+16z^2)$. We also adopt the LOD-MS II to solve the model under the mesh step size $h=0.16, \tau=0.01$. The profiles of the real part and imaginary part of the wave function at $z=3.2, t=3$ are shown in Fig. 6, and the residuals of mass and local energy are presented in Fig. 7.
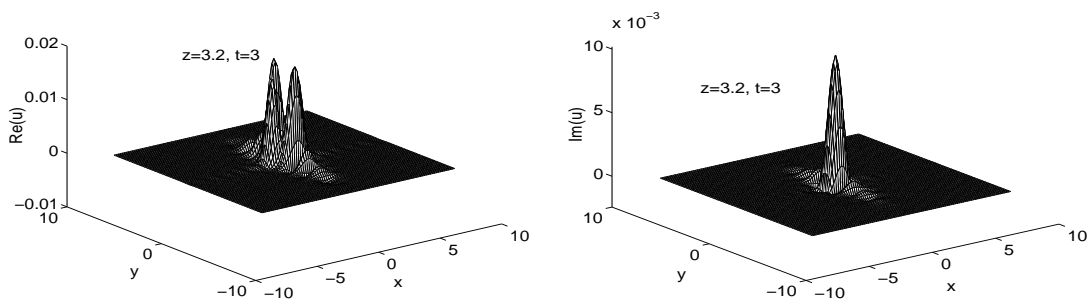
Figure 6: The real and imaginary parts of the wave function. Left: real; Right: imaginary.
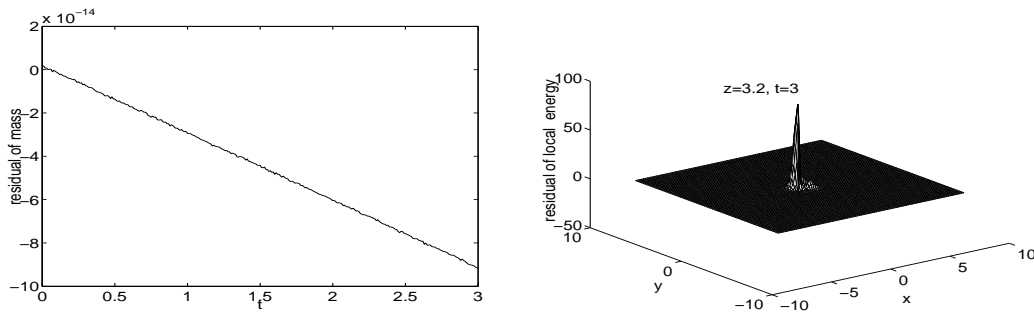
Figure 7: The residuals of mass and local energy. Left: mass; Right: local energy.

7   Conclusions and remarks

Combing the LOD thought with the MI, a novel and practical kind of MIs are developed for multidimensional Hamiltonian system. We call it LOD-MS. The method conserves the LOD MCLs and total symplectic structure. Under certain conditions, it also preserves global energy and local energy. Theoretical results are supported by numerical tests. Moreover, we can extend the method to other multidimensional Hamiltonian systems. We can also construct explicit or semi-explicit schemes for the systems. For example, we can apply partitioned RK to the LOD Hamiltonian system. These are our future work on the subject.

Acknowledgments

References

[1] A. Aydin, B. Karasözen, Lobatto IIIA-IIIB discretization of the strongly coupled nonlinear Schrödinger equation. J. Comput. Appl. Math., 235 (2011), pp. 4770-4779.
[2] W. Bao, Numerical methods for the nonlinear Schrödinger equation with nonzero far-field conditions, Methods and Applications Anal., 11 (2004), pp. 1-22.
[3] W. Bao, Q. Du, Computing the gounds state solution of Bose-Einstein Condensates by a normalized gradient flow, SIAM J. Sci. Comput., 25 (2004), pp. 1674-1697.
[4] W. Bao, Q. Du, Y.Z. Zhang, Dynamics of rotating Bose-Einstein Condensates and its efficient and accurate numerical computation, SIAM J. Appl. Math., 66 (2006), pp. 758-786.

[5] T.J. Bridges, S. Reich, Multi-symplectic integrators: numerical schemes for Hamiltoninan PDEs that conserve symplecticity, Phys. Lett. A, 284 (2001), pp. 184-193.

[6] J. Cai, Y. Wang, Z. Qiao, Multisymplectic Preissman scheme for the time-domain Maxwell's equations, J. Math. Phys., 50 (2009), pp. 033510.

[7] F. Dalfovo, S. Giorgini, Theory of Bose-Einstein condensation in trapped gases, Rev. Mod. Phys., 71 (1999), pp. 463-512.

[8] Q. Du, L. Ju, Numerical simulations of the quantized vortices on a thin superconducting hollow sphere, J. Comput. Phys., 201 (2004), pp. 511-530.

[9] E.P. Gross, Hydrodynamics of a superfluid condensate, J. Math. Phys., 4 (1963), pp. 195.

[10] E. Hairer, C. Lubich, G. Wanner, Geometric Numerical Integration Structure-preserving Algorithms for Ordinary Differential Equations, 2nd ed., Springer-Verlag, Berlin, 2006.

[11] J. Hong, L. Kong, Novel multi-symplectic integrators for nonlinear fourth-order Schrödinger equation with a trapped term, Commun. Comput. Phys., 7(2010), pp. 613-630.

[12] J. Hong, X. Liu, C. Li, Multi-symplectic Runge-Kutta-Nyström methods for nonlinear Schrödinger equations with variable coefficients, J. Comput. Phys., 226 (2007), pp. 1968-1984.

[13] H. Huang, L. Wang, Local one-dimensional multisymplectic integrator for Schröinger equation, J. Jiangxi Normal. Univer., 35 (2011), pp. 455-458.

[14] A.L. Islas, C.M. Schober, Multi-symplectic methods for generalized Schrödinger equations, Future Gener. Comput. Syst., 19 (2003), pp. 403-413.

[15] L. Kong, J. Hong, J. Zhang, Splitting multi-symplectic methods for Maxwell's equation, J. Comput. Phys., 229 (2010), pp. 4259-4278.

[16] K.W. Morton, D. F. Mayers, Numerical solution of partial differential equations, Cambridges University Press: Cambridge, 2005.

[17] D. Peaceman, H. Rachford, The numerical solution of parabolic and elliptic equations, J. Soc. Indust. Appl. Math., 3 (1955), pp. 28-41.

[18] L.P. Pitaevskii, Vortex lines in an imperfect Bose gas, Zh. Eksp. Teor. Fiz. 40 (1961), pp. 646.

[19] S. Reich, Multi-symplectic Runge-Kutta collocation methods for Hamiltonian wave equation, J. Comput. Phys., 157(2000), pp. 473-499.

[20] P.A. Ruprecht, M.J. Holland, K. Burrett, M. Edwards, Time-dependent solution of the nonlinear Schrödinger equation for Bose-condensed trapped neutral atoms, Phys. Rev. A, 51 (1995), pp. 4704-4711.

[21] G. Strang, On the construction and comparison of difference schemes. SIAM J. Numer. Anal., 5 (1968), pp. 506-517.

[22] F. Tappert, Numerical solutions of the Korteweg-de Vries equation and its generalizations by the split-step Fourier method. in: A.C. Newell(Ed.), Nonlinear Wave Motion, Lect. Appl. Math., Amer. Math. Soc., Providence, RI, 15 (1974) 215-216.

[23] Y. Tian, M. Qin, Y. Zhang, T. Ma, The multisymplectic numerical method for Gross-Pitaevskii equation, Comput. Phys. Commun., 178 (2008), pp. 449-458.

[24] H. Wang, Numerical studies on split-step finite difference method for nonlinear Schrödinger equations, Appl. Math. Comput., 170 (2005), pp. 17-35.

[25] L. Wang, Multisymplectic Preissman scheme and its application. J. Jiangxi Normal Univer. 33 (2009), pp. 42-46.

[26] J. Zhang, Z. Xu, X. Wu, Unified approach to split absorbing boundary conditions for nonlinear Schrödinger equations: Two-dimensional case. Phys. Rev. E, 79 (2009), pp. 046711.

[27] Y. Zhang, Numerical study of vortex interactions in Bose-Einstein condensation. Commun. Comput. Phys., 8 (2010), pp. 327-350.